JJEE Volume X | Number X | Month 20XX | Pages XXX-XXX

Jordan Journal of Electrical Engineering

ISSN (print): 2409-9600, ISSN (online): 2409-9619

Homepage: jjee.ttu.edu.jo

Performance Analysis of BiCoRE Solar Cells under Variable Albedo Conditions

Tekkouk Adda Benattia[1*], Abdelkader Mekemeche[2]

[1] Physics Department, Faculty of Exact Sciences and Computer Science, Abdelhamid Ibn Badis University, Mostaganem, Algeria.

E-mail : tekkouk.addabenattia@univ-mosta.dz

[1] Electromagnetism and Guided Optics Laboratory (LEOG), Abdelhamid Ibn Badis University of Mostaganem, Algeria

[2] Civil Engineering Department, Faculty of Technology, Saad Dahlab University, Blida, Algeria

[2] Elaboration and Characterization of Physico-Mechanical and Metallurgical Materials Laboratory (ECP3M), Abdelhamid Ibn Badis University, Mostaganem, Algeria

Received: Dec 01, 2024 *Revised: Mar 02, 2025* *Accepted: Mar 14, 2025* *Available online: Apr 6, 2025*

***Abstract*—** This investigation examines the performance of BiCoRE (Bifacial Co-diffused Rear Emitter) solar cells under varying albedo conditions, focusing on critical performance parameters, namely short-circuit current density (J_{sc}), open-circuit voltage (V_{oc}), fill factor (FF), and output power (P_{out}). Using Personal Computer 3D (PC3D) software for detailed 3D modeling and dual-surface illumination simulations, we observed significant performance improvements under reflective surface conditions. For instance, on snow-covered surfaces, the output power increased from 20.69 mW/cm² to 34.41 mW/cm², marking a 66.31% improvement compared to front-side-only illumination. The investigation further models the relationship between albedo variations and the four key performance parameters of the BiCoRE cell. The resulting linear models demonstrate a robust correlation, enabling accurate predictions of cell performance across diverse albedo levels without the need for additional simulations. Comparisons between the linear models and the simulation results confirm strong alignment across all parameters. High albedo values, particularly in reflective environments, substantially boost energy output, emphasizing the importance of albedo as a pivotal factor for optimizing the energy efficiency of BiCoRE solar cells. These results highlight the potential of bifacial designs to enhance energy capture in a wide range of environmental scenarios.

***Keywords*—** Bifacial solar cells; BiCoRE solar cells; Albedo conditions; PC3D software; Simulation.

1. INTRODUCTION

Solar energy is an abundant and clean renewable resource with enormous potential to meet global energy needs. Bifacial solar cells stand out due to their innovative design, which enables the capture of light on both their front and rear surfaces. This unique feature significantly enhances energy efficiency, especially when installed on surfaces that reflect sunlight. By optimizing light collection from both sides, bifacial cells are able to capture some of the incident light that is reflected back onto the rear surface in environments such as urban areas, water bodies, or snow-covered ground. This reflected light is then converted into electricity, increasing the overall power output of the cell [1].

The initial bifacial solar cell experiment, achieving a modest 7% efficiency, was introduced in 1977 at the inaugural European Conference on Photovoltaic Solar Energy in Luxembourg [2, 3]. In the same year, R. J. Schwartz and M. D. Lammert [4] explored the design of the Interdigitated Back Contact (IBC) solar cell, where both *p*-type and *n*-type electrodes are

* Corresponding author

DOI: https://doi.org/10.5455/jjee.204-1733039221

placed on the rear side of the cell. This allows the entire front surface to be exposed to light, maximizing light absorption. In 1978, the IBC design was superseded by a homopolar junction (front surface field) structure. These early innovations inspired the invention of bifacial solar cells [5, 6].

Bifacial solar cells can be categorized into three distinct types based on the number and position of the PN junctions in their structure [6]. The first structure, proposed by Japanese researcher Hiroshi Mori in 1960, was named "Bifacial Cells with Double Junction" [7]. This structure offers better collection of longer wavelengths (absorbed near the rear for front-incident light) and allows the use of low-quality substrates (such as *p*-type material with low diffusion lengths), though its manufacturing process is more complex [8]. The second structure, referred to as bifacial back surface solar cells, has a specific design that includes a homopolar pp+ (or nn+) junction on the cell's rear surface. This junction is positioned opposite the heteropolar p-n junction located on the front surface [9]. The third structure, introduced by Chevalier and Chambouleyron in 1977, is characterized by a rear metal grid that makes contact with the substrate, while the rest of the rear surface is passivized and left unmetallized [10]. This structure is commonly known as the passivated emitter and rear contact solar cell (PERC).

Recent advancements in solar cell technology have resulted in the creation of passivated emitter rear totally diffused cells (PERT). These cells are produced using a process similar to that of PERC cells, but they feature distinct improvements, including boron doping on the rear side and larger passivation layers. PERT cells have garnered interest for their potential to improve efficiency when combined with n-type substrates. While light-induced degradation (LID) continues to limit the conversion efficiency of p-PERC cells, despite advances in industrial regeneration processes, n-PERT back junction (BJ) cells are emerging as a promising alternative. Many p-PERC solar cell manufacturers are considering transitioning their production from p-type wafers to n-type wafers[11, 12].

In recent years, T. Dullweber introduced an innovative solar cell design called BiCoRE (Bifacial Codiffused Rear Emitter), focused on enhancing energy efficiency and addressing the efficiency degradation issues common in traditional cells. This design builds upon and improves the performance of PERC and n-PERT cells. By incorporating a borosilicate glass (BSG) and silicon nitride (SiNx) layer for effective passivation, the BiCoRE design offers notable benefits. It leverages n-type silicon wafers to eliminate light-induced degradation (LID), a frequent issue in *p*-type cells, and integrates aluminum rear grids to enhance bifacial performance, maximizing energy generation under favorable conditions. Notably, BiCoRE cells demonstrate a front-side efficiency of 20.6% and a rear-side efficiency of 16.1%, achieving a bifaciality of 78%.

BiCoRE technology stands out for its high bifaciality factor and compatibility with existing production lines. However, it still lacks field data and long-term reliability studies. Compared to established technologies like PERC (high efficiency and low cost), n-PERT (excellent temperature coefficient), and HJT (very high efficiency but high manufacturing costs), BiCoRE remains a promising but evolving solution that requires further research to confirm its long-term competitiveness. The cost of these cells primarily depends on the materials used (SiNx, BSG, aluminum) and their integration into existing industrial processes, offering a balance between efficiency and production costs. [13].

The performance of bifacial solar cells is strongly influenced by environmental factors, particularly the albedo of reflective surfaces[6, 14-17].This study aims to investigate the impact of various reflective surfaces on enhancing the energy efficiency of BiCoRE (Bifacial Co-Diffused Rear Emitter) solar cells by simulating, modeling, and analyzing the effect of albedo on electrical parameters such as short-circuit current density (J_{sc}), open-circuit voltage (V_{oc}), fill factor (FF), and output power (P_{out}).This research highlights the importance of environmental albedo in optimizing the performance of bifacial solar cells on various common surfaces [18]. Using the PC3D simulator, we model this effect on BiCoRE cells to provide a predictive tool that helps adapt these cells to the most favorable environmental conditions, thereby maximizing their energy efficiency.

2. BICORE SOLAR CELLS STUCTURE

BiCoRE solar cells represent advancement in crystalline silicon solar cells designed to enhance solar energy conversion efficiency. The manufacturing process of these cells typically involves several key stages. The depicted, in Fig. 1, BiCoRE solar cell is a 156x156 mm^2 pseudo-square *n*-type bifacial cell created using phosphorus-doped monocrystalline silicon wafers produced through the Czochralski process, exhibiting a resistivity of 6.5 Ω.cm.

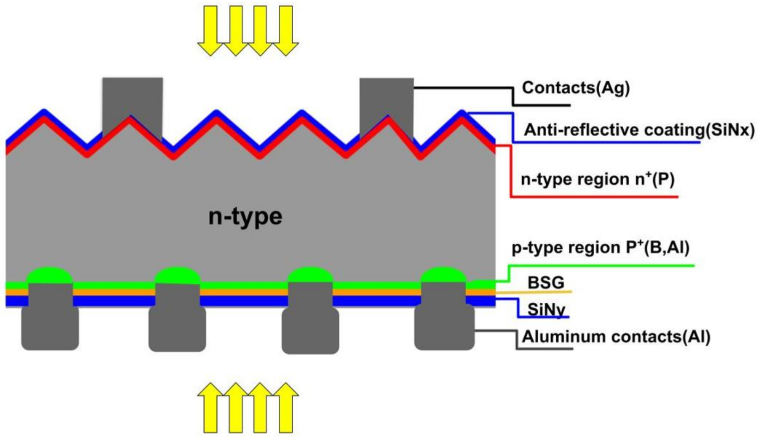

Fig. 1. Schematic diagram of the bifacial solar cell "BiCoRE".

The manufacturing process for BiCoRE cells comprised ten consecutive steps as exhibited in Fig. 2. Initially, the wafers underwent cleaning, followed by the application of the BSG/SiNy stack onto the rear surface using the PECVD (Plasma-Enhanced Chemical Vapor Deposition) method. This passivation layer helps reduce recombination losses. Subsequently, an alkaline texturing process was employed on the front surface to improve light absorption by reducing light reflection from the cell surface. Co-diffusion of $POCL_3$ (trichlorophosphine oxide) was then employed on the front surface to introduce phosphorus (P) into a superficial silicon (Si) layer, creating a doped *n*-region (*n*+).

Due to the SiNy passivation layer on the back, only the front face of the wafer is textured and doped with phosphorus. The PSG (Phosphosilicate glass) layer on the front face of the wafer is removed by a brief immersion in HF (hydrofluoric acid), however, this does not remove the BSG/SiNy stack on the back of the wafer. Next, we deposit a SiNx (PECVD) anti-reflective coating on the front face of the wafer.

The rear contacts are formed by laser ablation with optimal LCO (Laser Contact Opening) widths of 40 µm and a pitch of 1270 µm. The front silver contacts are double-printed, and the rear aluminum finger grid is screen-printed using a finger opening of 100µm. The process concludes with the firing of the solar cell at its optimal firing temperature [13] .

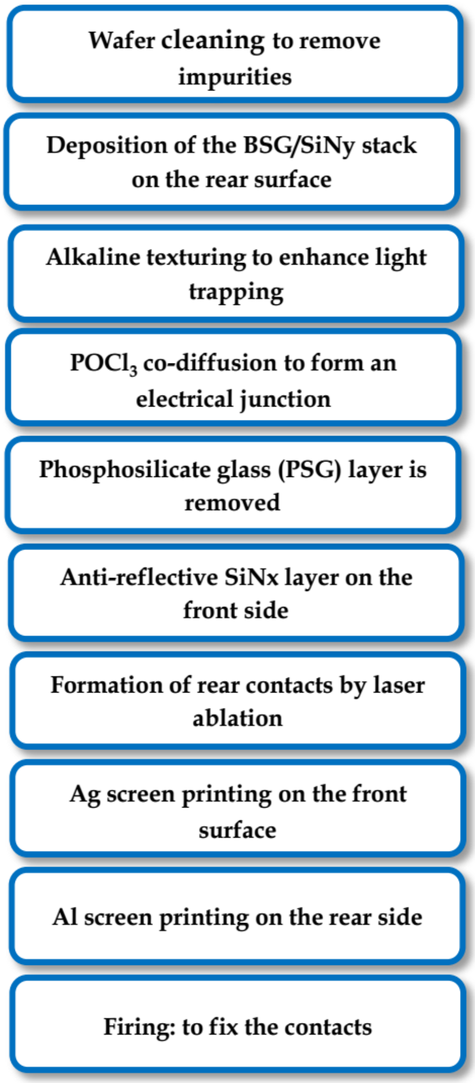

Fig. 2. BiCoRE solar cell manufacturing steps.

3. NUMERICAL MODELING AND SIMULATION

The BiCoRE solar cell was simulated using the PC3D numerical simulator, based on solving the drift-diffusion equations. Unlike 1D solutions that use Poisson's equation, 3D solutions, though more complex, offer advantages such as representing edge effects. In 2010, R. Brendel et al [19] recognized that for silicon wafer solar cells, the near-surface region containing texture, heavy doping, and space charge can be mathematically treated as a thin sheet boundary condition when solving the drift-diffusion equations within the bulk of the wafer.

This insight enabled the rapid development of multidimensional solar cell device modeling software, freely available for personal computers, starting with PC2D for 2D modeling, followed by Quokka2 for 3D modeling. Recently, PC3D was released, which differs from the others mainly by using the multidimensional solution method of Fourier series. Our aims are to model and simulate the impact of environmental albedo on the energy efficiency of BiCoRE solar cells with simultaneous illumination on both sides.

Multidimensional device simulators leverage the fact that electron and hole densities in the wafer bulk are nearly equal, differing by less than one part per million. This minor discrepancy has a significant impact on the electric field and currents. To determine the electric field under steady-state conditions, the "quasi-neutral" approximation is employed, treating the excess electron and hole densities as equal. Gamma (Γ) represents this excess density, while psi (Ψ) denotes the excess potential. Both Γ and Ψ are functions of the spatial coordinates x, y, and z. A complete solution for the electron and hole densities in the quasi-neutral volume is provided by the functions Γ(x, y, z) and Ψ(x, y, z), which satisfy the quasi-neutral approximation of the drift-diffusion equations. Boundary conditions are applied to the front and back surfaces, as well as the edges along the x and y axes. In terms of Γ and Ψ, the current densities of the hole vector (p) and the electron (n) in a uniformly doped quasi-neutral material are described by [20]:

$$J_n = +qD_n\nabla\Gamma - qD_n(n_{eq}+\Gamma)\nabla\Psi / V_t \tag{1}$$

$$J_p = -qD_p\nabla\Gamma - qD_p(p_{eq}+\Gamma)\nabla\Psi / V_t \tag{2}$$

where D_n and D_p are respectively the diffusivities of holes and electrons (assumed uniform), P_{eq} and n_{eq} are the uniform equilibrium concentration of holes and electrons, q is the positive elementary charge and V_t (KT/q) is the thermal tension ($V_t = 25.69$ mV at 25°C). The continuity of holes and electrons in a steady state requires that:

$$\nabla.\vec{J}_n = +q(R-G) \tag{3}$$

$$\nabla.\overrightarrow{J_p} = -q(R-G) \tag{4}$$

where R is the local recombination rate (a function of *Γ*, but not of *Ψ*), and *G* is the local photogeneration rate (independent of both *Γ* and *Ψ*). Note that as long as Eq. (3) and Eq. (4) are satisfied, the continuity of the total current density $\nabla.J_{tot}=0$ is ensured [20, 21].

The semiconductor drift-diffusion equations are simplified to two variables using the quasi-neutral approximation. These equations are solved using Fourier-series techniques, especially for symmetric solar cells. Implemented in PC3D, this method generates precise (J-V) curves quickly on standard PC.

4. ANALYSIS OF RESULTS AND SIMULATION

4.1. Simulation and Results with AM1.5G

To simulate the BiCoRE cell developed by T. Dullweber using PC3D, we utilized the experimental parameters listed in Table 1. The simulation results, presented in Table 2, were compared with the experimental data, revealing a strong correlation, as noted in [13, 22]. The minor discrepancies between simulated and experimental values can be attributed to asymmetries in the simulation region and approximations of certain physical parameters. Nevertheless, this initial validation phase confirms the reliability of the PC3D simulator for studying BiCoRE cells and paves the way for a more in-depth modeling of the impact of albedo on their energy efficiency. Although our PC3D simulations have shown a strong correlation with experimental data, some limitations remain. In particular, approximations in accounting for surface effects and spectral variations of albedo may lead to discrepancies with real measurements. Additionally, the long-term stability of cell performance under real-world conditions has not yet been experimentally validated. Further studies, including extended outdoor testing, would be necessary to refine the accuracy of the models and better predict the long-term performance of BiCoRE cells in practical applications.

Table 1. General BiCoRE solar cell simulation input parameters [13, 23, 24].

Front	Bulk	Rear
Sheet resistance(n+):130 Ω/□ Pitch: 2.54 mm Finger width: 70 μm Busbars number: 5 Busbar width: 540 μm	Thickness: 170 μm Resistivity: 6.5 Ω.cm Lifetime (n-type): $\tau_n = \tau_p$ =10 ms	Local BSF (p+) :100 Ω/□ Pitch: 1.27 mm Finger width: 100 μm Busbars number: 5 Busbar width: 540 μm

Table 2. Simulation results of the BiCoRE solar cell (front/rear) with AM1.5G.

Result	Illumination side	J_{sc} [mA/cm²]	V_{oc} [mV]	FF [%]	P_{out} [mW/cm²]
Simulation	Front	39.30	668.58	78.70	20.70
	Rear	31.18	663.14	79.40	16.41
Experimental [13]	Front	39.30	669.00	78.40	20.60
	Rear	30.70	663.00	79.10	16.10

Figs. 3 (a) and (b) present the simulated BiCoRE solar cell's short-circuit current density (J_{sc},V) and power (P_{out},V) curves, derived from the parameters listed in Table 1. These curves are shown separately for the front and rear sides, providing a detailed performance comparison of each side. The results indicate that the rear-side short-circuit current density is 79.33% of the front side, while the open-circuit voltage on the rear side reaches 99.93% of the front side. This corresponds to a bifaciality factor of 80% in terms of power output.

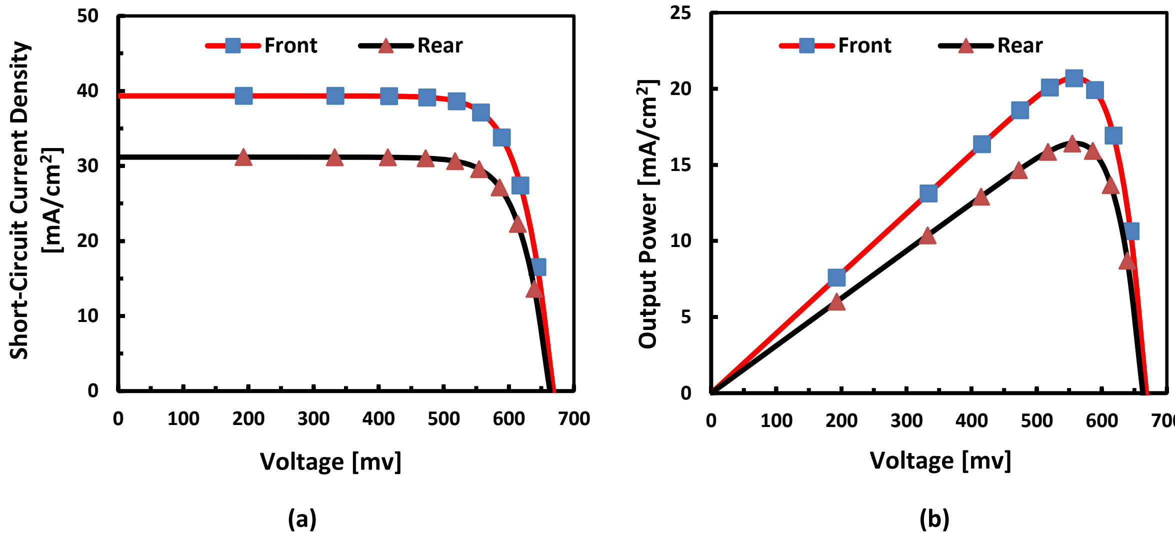

Fig. 3. Characteristics of the simulated BiCoRE solar cell (front and rear): a) short-circuit current density versus tension; b) output power versus tension

4.2. Impact of Albedo on the Efficiency of BiCoRE Solar Cells

The advantage of bifacial solar cells is the use of light from both sides at the same time. With a normalized power of 1000 W/m², the front face is exposed to the overall radiation of the AM1.5G spectrum, while the back face receives the albedo or reflected light from the surface below. The characteristics of this surface significantly influence the output power as well as the efficiency. The spectral albedo of a surface describes how its reflectance varies with different wavelengths of light. In our simulation, we chose seven common surfaces: green grass, white sand, red brick, roof shingles, dry grass, building concrete, and snow. The spectral albedo data used were obtained from the Advanced Space borne Thermal Emission and

Reflection Radiometer (ASTER) spectral library version 2.0 of the Jet Propulsion Laboratory[25].

The (J_{sc},V) characteristics of the equivalent BiCoRE cell, when illuminated simultaneously from both surfaces, show improved overall performance with the effective surface albedo described earlier. Based on these characteristics, we can infer the variation of the four parameters (J_{sc}, V_{oc}, FF, and P_{out}) of the equivalent cell as a function of the effective albedo of each surface; the results are presented in the following Table (Table. 3).

Table 3. Simulation results for the parameters of the BiCoRE cell under varying Albedo values.

Surface albedo	Albedo value	J_{sc} [mA/cm²]	V_{oc} [mV]	FF [%]	P_{out} [mW/cm²]
Black surface	0	39.33	668.58	0.78	20.69
Green grass	0.24	46.82	673.18	0.78	24.63
Roofing shingle	0.26	47.45	673.53	0.78	24.96
Construction concrete	0.29	48.38	674.04	0.78	25.45
Dry grass	0.44	53.06	676.46	0.77	27.86
White sand	0.67	60.24	679.77	0.77	31.56
Snow	0.85	65.86	682.09	0.76	34.41
AM1.5G	1	70.54	683.86	0.76	36.77

4.2.1. *Impact of Albedo on the Short-Circuit Current Density*

It is clear – from Fig. 4 - that the short-circuit current density (J_{sc}) increases linearly with the effective albedo. For example, it ranges from 39.33 mA/cm² (black surface) to 65.54 mA/cm² (snowy surface). This increase is expected, as an increase in incident power leads to greater photo generation. This result aligns with the theoretical relationship between current and irradiance in photovoltaic cells, where the photocurrent generated in the solar cell is directly proportional to the intensity of the incident solar radiation. This relationship can be expressed as:

$$J_{ph} = q\eta_{opt}G \tag{5}$$

where J_{ph} is the photocurrent [A/cm²], q is the charge of an electron (1.6×10^{-19} C), η_{opt} is the optical efficiency (accounting for losses such as reflection and transmission), and G is the irradiance [W/cm²].

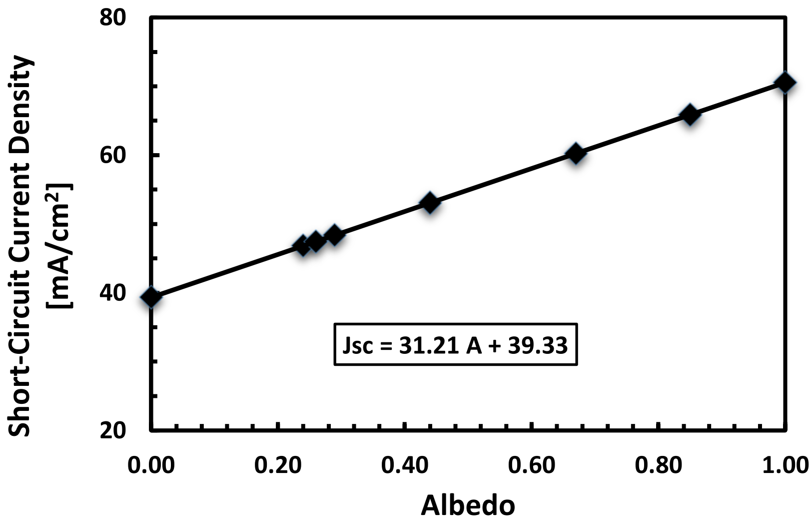

Fig. 4. Short-circuit current density versus albedo.

Eq. (6) demonstrates that the photocurrent increases linearly with irradiance, assuming the optical efficiency remains constant [26]. The (J_{sc}), which is the current produced when the solar cell's terminals are short-circuited, is directly proportional to irradiance. This relationship can be expressed as:

$$J_{sc} = J_{sc.ref} \frac{G}{G_{ref}} \tag{6}$$

where $J_{sc.ref}$ is the short-circuit current at a reference irradiance J_{ref} , and G is the actual irradiance. So, theoretically, the J_{SC} increases linearly with increasing irradiance.

4.2.2. Impact of Albedo on the Open-Circuit Voltage

The effect of albedo on the (V_{oc}) of a bifacial solar cell is tied to how albedo influences the photo-generated current (I_{ph}). Since Voc is related to I_{ph}, any increase in I_{ph} due to higher albedo will impact V_{oc} as well. Fig. 5 shows that the (V_{oc}), which represents the maximum voltage when no current is drawn from the cell, has a nearly linear relationship with the radiation and thus with the albedo for our bifacial cell named BiCoRE. These results are consistent with the theoretical relationships after the approximations. The open circuit voltage (Voc) is given by the following theoretical relation [8].

$$V_{oc} = \frac{nKT}{q} \ln(\frac{I_{ph}}{I_0} + 1) \tag{7}$$

where I_{ph} is the photo-generated current,I_0 is the diode saturation current, n is the diode ideality factor, K is the Boltzmann constant, T is the absolute temperature, an and q is the electron charge. When the term $I_{ph} / I_0 >> 1$ which is typically the case under standard operating conditions (as I_0 is small and I_{ph} is large under illumination), we can approximate the logarithm as follows:

$$V_{oc} = \frac{nKT}{q} \ln(\frac{I_{ph}}{I_0}) \tag{8}$$

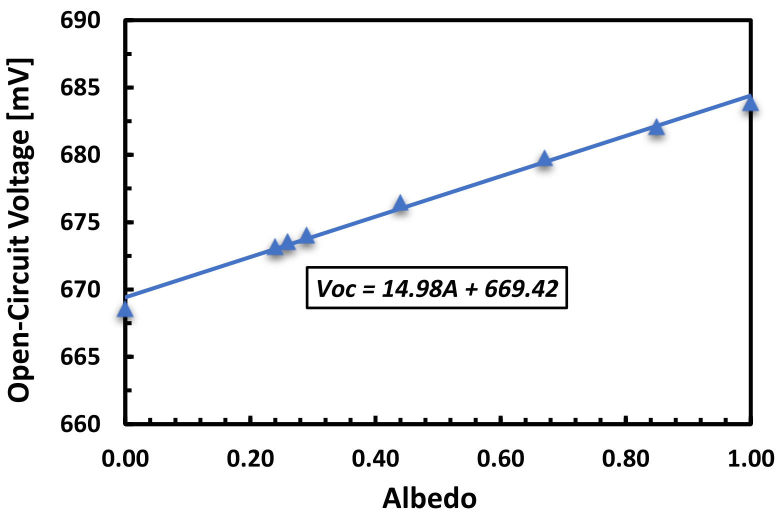

Fig. 5. Open circuit voltage versus albedo.

Since V_{oc} depends logarithmically on I_{ph} an increase in albedo (which increases I_{ph}) will cause a slight rise in the open-circuit voltage. However, this effect is less pronounced compared to the impact on current I_{sc} due to the logarithmic relationship. This shows that V_{oc} increases slowly between (668.58- 683.86 mV) with rising irradiance, in contrast to the short-circuit current density, which responds more strongly. In our study of the BiCoRE bifacial cells with an albedo range of 0 to 1 (irradiance between 1000 and 2000), the relationship between V_{oc} and I_{ph} can be approximated as linear (see Fig. 5). This simplifies the analysis of Voc within this irradiance range, considering the influence of albedo.

4.2.3. Impact of Albedo on the Output Power

Fig. 6 illustrates the simulation results showing the evolution of (P_{out}) as a function of albedo. It is clear that the power increases linearly with rising albedo[27], a behavior consistent with the physical properties of the bifacial cell, which captures both direct radiation and reflected light from the environment [28].

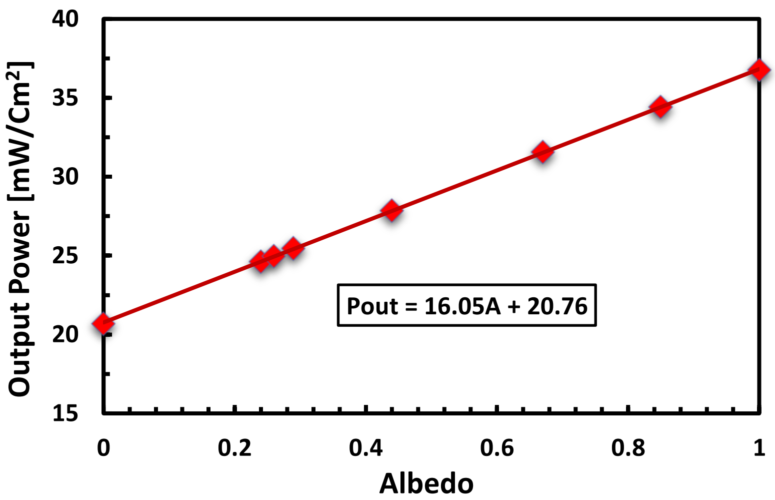

Fig. 6. Output power versus albedo.

This trend aligns with the theoretical relationship described as follows:

$$P_{out} = \eta G(1 + A) \tag{9}$$

where η represents the solar cell's conversion efficiency, G is the irradiance directly from sunlight, and A is the albedo.

4.2.4. Impact of Albedo on the Fill Factor

According to Eq. (10), the FF remains almost constant with increasing albedo [29]. Indeed, the effect of increasing albedo mainly affects (J_{sc}) as we proved in the previous paragraph, while its effect on the (FF) is small and indirect as shown in Fig. 7. This stability is due to the logarithmic relationship between J_{SC} and V_{OC} on the one hand and FF and V_{oc} on the other hand, which makes the effect of albedo on the fill factor negligible.

Therefore, even when albedo varies, (FF) only shows slight fluctuations, maintaining relative stability.

$$FF = \frac{V_{oc} - \frac{K_B T}{q}\ln\left(\frac{qV_{oc}}{K_B T} + 0.27\right)}{V_{oc} + \frac{K_B T}{q}} \tag{10}$$

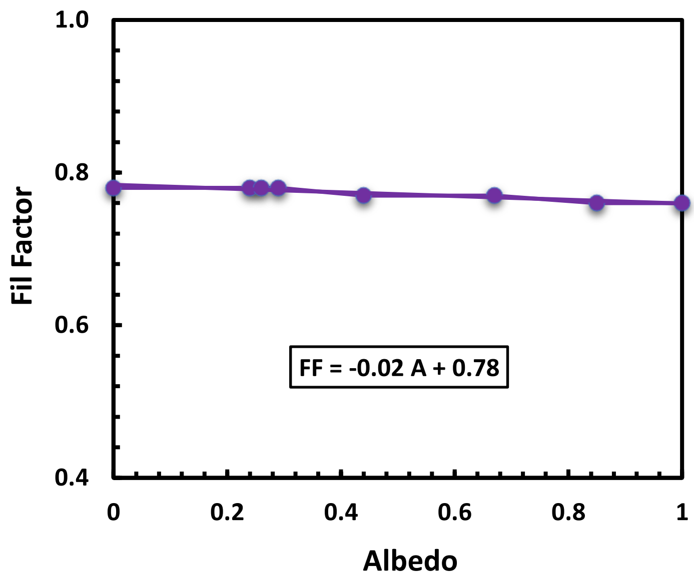

Fig. 7. Fill factor versus albedo.

By using this estimation method, solar cell performance can be predicted for different albedo levels without additional simulations. This simplifies the design and optimization of photovoltaic devices. Solar cells can thus adapt to various environmental conditions, enhancing their energy efficiency and cost-effectiveness.

To validate our modeling of these parameters (Eq. 11), we tested our BiCoRE cell with two surfaces not included in the initial study, such as white paint and aluminum, with albedos of 0.42 and 0.54, respectively [14]. The results are presented in the following tables:

$$J_{sc} = 31.21A + 39.33 \quad (11.a)$$

$$V_{oc} = 14.98A + 669.42 \quad (11.b)$$

$$P_{out} = 16.06A + 20.76 \quad (11.c)$$

$$FF = -0.02A + 0.78 \quad (11.d)$$

Tables (4) and (5) present the simulation results obtained using PC3D and the mathematical model based on a first-order linear equation (Eq. 11 (a-d)). A complete agreement is observed between the results from both approaches. This study offers significant advantages, aiding in the optimal selection of locations for bifacial solar panels, particularly in high-albedo environments such as snowy or desert areas, thereby maximizing energy yield and return on investment [30].

Additionally, the linear model simplifies performance estimation for engineers, reducing reliance on complex simulations and accelerating the planning process, which enhances the economic feasibility of solar projects. In the future, the validity of this model can be further confirmed by comparing these results with experimental data, which are not yet available, as BiCoRE cells remain at the experimental stage.

Table 4. Results obtained by PC3D simulation.

Surface Albedo	Albedo value [A]	J_{sc} [mA/cm^2]	V_{oc} [mV]	FF	P_{out} [mW/cm^2]
White paint	0.42	52.44	676.17	0.77	27.55
Aluminum	0.54	56.18	677.97	0.77	29.48

Table 5. Results obtained by linear modeling.

Surface Albedo	Albedo value [A]	J_{sc} [mA/cm^2]	V_{oc} [mV]	FF	P_{out} [mW/cm^2]
White paint	0.42	52.44	675.71	0.77	27.50
Aluminum	0.54	56.18	677.50	0.77	29.43

5. CONCLUSIONS

The PC3D software enables the modeling of bifacial solar cells with simultaneous illumination on both surfaces and simulating the (J-V) characteristics of BiCoRE cells and determining key performance parameters (J_{sc}, V_{oc}, FF, and P_{out}) based on the effective albedo for the various surfaces including Black surface, green grass, roofing shingles, construction concrete, dry glass, white sand, and snow.

In this paper, firstly, we validated the PC3D simulation by comparing our results with the experimental data for both sides of the BiCoRE cell, focusing on J_{sc}, V_{oc}, P_{out}, and FF parameters, which were found to be in agreement. In the second step, we simulated the impact of albedo on the parameters of the studied cell (BiCoRE). We observed that the J_{sc} increases linearly with effective albedo due to enhanced incident power, which boosts photogeneration. Consequently, the V_{oc} also rises, though at a slower rate. In contrast, the FF remains nearly constant, as its logarithmic dependence on J_{sc} and V_{oc} minimizes the impact of albedo variations. As a result, the P_{out} follows a proportional increase with albedo, highlighting the significant influence of reflected radiation on bifacial solar cell performance.

This observed linearity allowed us to model the parameters (J_{sc}, V_{oc}, FF, and P_{out}) as first-degree equations based on effective albedo, facilitating the optimization of bifacial solar cell design and deployment. By understanding how different surface albedos affect performance, informed decisions can be made to maximize energy yield and predict long-term performance in various environments, facilitating strategic panel placement in high-reflectivity areas such as snow, sand, or near reflective roofs. The development of a linear model reduces design complexity and costs while improving energy efficiency, enhancing the feasibility and economic viability of solar projects.

However, this study has certain limitations. The simulations were conducted under idealized conditions and have not been extensively validated in real-world environments. Factors such as spectral variations of reflected light, temperature effects, shading, and long-term degradation were not fully accounted for. Additionally, the model's applicability to large-scale installations and diverse geographic regions requires further investigation. Future work should focus on experimental validation under real-world conditions, exploring a wider range of surface types, and assessing long-term durability to confirm the model's accuracy and adaptability. These efforts will advance the industrial deployment of BiCoRE solar cells and contribute to the broader adoption of bifacial photovoltaic technologies, supporting the global transition to sustainable energy solutions.

Acknowledgement: The authors extend their sincere gratitude to Mr. Paul A. BASORE, IEEE member, for his invaluable guidance in programming with PC3D software. His clear and prompt responses to the authors’ inquiries greatly assisted in utilizing the simulator effectively.

REFERENCES

[1] N. Asgher, T. Iqbal, "Design and simulation of a floating solar photovoltaic system for an offshore aquaculture site in Canada," *Jordan Journal of Electrical Engineering*, vol. 9, no. 4, pp. 466–480, 2023, doi: 10.5455/jjee.204-1688997421.

[2] C. Duran, P. Hering, T. Buck, K. Peter, "Characterization of bifacial silicon solar cells and modules: a new step," European Photovoltaic Solar Energy Conference Eupvsec, 2011.

[3] C. Duran, "Bifacial Solar cells: high efficiency design, characterization, modules and applications," *University of Konstanz*, 2012, http://nbn-resolving.de/urn:nbn:de:bsz:352-205361.

[4] M. Lammert, R. Schwartz, "The Interdigitated back contact solar cell: a silicon solar cell for use in concentrated sunlight," *IEEE Transaction on Electron Devices*, vol. ED-24, no. 4, pp. 337–342, 1977, doi: 10.1109/T-ED.1977.18738.

[5] A. Cuevas, "The early history of bifacial solar cells," European Photovoltaic Solar Energy Conference, 2005.

[6] A. Mekemeche, M. Beghdad, "Impact of the environmental effective albedo on the performance of PERC + solar cells," *Silicon*, vol. 13, no. 11, pp. 3991–3998, 2021, doi: 10.1007/s12633-020-00707-8.

[7] H. Mori, "Radiation energy transducing device," *United States Patent*, 1961, https://patents.google.com/patent/US3278811A/en.

[8] B. Soria, " Annual electrical performances of bifacial photovoltaic modules. Case study vertical facade integration of bifacial modules.," *University of Grenoble*, 2014, https://theses.hal.science/tel-01126959

[9] A. Cuevas, A. Luque, J. Eguren, J. Alamo, "High efficiency bifacial back surface field solar cells," *Solar Cells*, vol. 3, no. 4, pp. 337–340, 1981, doi: 10.1016/0379-6787(81)90024-7.

[10] A. Blakers, "Development of the PERC solar cell," *IEEE Journal of Photovoltaics*, vol. 9, no. 3, pp. 629–635, 2019, doi: 10.1109/JPHOTOV.2019.2899460.

[11] N. Wehmeier , A. Nowack , B. Lim, T. Brendemühl, S. Kajari-Schröder, J. Schmidt, R. Brendel, T. Dullweber, "21.0%-efficient screen-printed n-PERT back-junction silicon solar cell with plasma-deposited boron diffusion source," *Solar Energy Materials and Solar Cells*, vol. 158, no. 1, pp. 50–54, 2016, doi: 10.1016/j.solmat.2016.05.054.

[12] J. Benick, B. Hoex, G. Dingemans, "High-efficiency n-type silicon solar cells with front boron emitter," European Photovoltaic Solar Energy Conference, 2009.

[13] T. Dullweber, N. Wehmeier, A. Nowack, T. Brendemühl, S. Kajari-Schröder, R. Brendel, "Industrial bifacial n-type silicon solar cells applying a boron co-diffused rear emitter and an aluminum rear finger grid," *Physical Status Solidi*, vol. 213, no. 11, pp. 3046–3052, 2016, doi: 10.1002/pssa.201600346.

[14] K. Ganesan, D. Winston, S. Sugumar, S. Jegan, "Performance analysis of n-type PERT bifacial solar PV module under diverse albedo conditions," *Solar Energy*, vol. 252, pp. 81–90, Mar. 2023, doi: 10.1016/j.solener.2023.01.020.

[15] S. Wallner, M. Kocifaj, "Impacts of surface albedo variations on the night sky brightness – a numerical and experimental analysis," *Journal of Quantitative Spectroscopy and Radiative Transfer*, vol. 239, p. 106648, 2019, doi: 10.1016/j.jqsrt.2019.106648.

[16] T. Russell, R. Saive, A. Augusto, S. Bowden, H. Atwater, "The influence of spectral albedo on bifacial solar cells: a theoretical and experimental study," *IEEE Journal of Photovoltaics*, vol. 7, no. 6, pp. 1611–1618, 2017, doi: 10.1109/JPHOTOV.2017.2756068.

[17] A. Goswami, "Effect of humidity on the generation capacity of floating solar photovoltaic system," *Jordan Journal of Electrical Engineering*, vol. 9, no. 1, pp. 31–41, 2023, doi: 10.5455/jjee.204-1667584023.

[18] J. Westerhof, L. Horst, A. Rikhof, S. Pal, D. Busko, B. Richards, R. Saive, "Impact of grass retroreflection on bifacial solar panel electricity yield in agrivoltaics," *Journal of Photonics Energy*, vol. 15, no. 3, pp. 1–10, 2025, doi: 10.1117/1.JPE.15.032702.

[19] R. Brendel, "Modeling solar cells with the dopant-diffused layers treated as conductive

boundaries," *Progress in Photovoltaics*, vol. 20, no. 1, pp. 6–11, 2012, doi: 10.1002/pip.954.

[20] P. Basore, "Multidimensional fourier-series solution of the quasi-neutral drift – diffusion equations," *IEEE Journal of Photovoltaics*, vol. 10, no. 3, pp. 905–911, 2020, doi: 10.1109/JPHOTOV.2020.2966831.

[21] N. Boukortt, B. Hadri, "Bifacial n-PERC solar cell characterization," *Indian Journal of Physics*, vol. 93, no. 1, pp. 33–39, 2019, doi: 10.1007/s12648-018-1274-5.

[22] N. Wehmeier, A. Nowack, "BiCoRE : combining a PERC-type cell process with n-type wafers," I*nstitute for Solar Energy Research Hamelin (ISFH), Emmerthal, Germany*, 2016, 838d9337aa-bicore-combining-a-perctype-cell-process-with-ntype-wafers.pdf.

[23] A Fell, K. McIntosh, P. Altermatt, G. Janssen, R. Stangl, A. Baillie, "Input parameters for the simulation of silicon solar cells in 2014," *IEEE Electron Devices Society,* vol. 5, no. 4, pp. 1250 - 1263, 2015, , doi: 10.1109/JPHOTOV.2015.2430016.

[24] T. Dullweber , M. Stöhr , C, Kruse , F. Haase , M. Rudolph, B. Beier , P. Jäger , V. Mertens , R. Peibst, R. Brendel, "Evolutionary PERC+ solar cell efficiency projection towards 24% evaluating shadow-mask-deposited poly-Si fingers below the Ag front contact as next improvement step," *Solar Energy Materials and Solar Cells*, vol. 212, 2020, doi: 10.1016/j.solmat.2020.110586.

[25] A. Baldridge, S. Hook, C. Grove, G. Rivera, "The ASTER spectral library version 2.0," *Remote Sensing of Environment*, vol. 113, no. 4, pp. 711–715, 2009, doi: 10.1016/j.rse.2008.11.007.

[26] M. Chegaar, A. Hamzaoui, A. Namoda, P. Petit, M. Aillerie, A. Herguth, "Effect of illumination intensity on solar cells parameters," *Energy Procedia*, vol. 36, pp. 722–729, 2013, doi: 10.1016/j.egypro.2013.07.084.

[27] U. Yusufoglu, T. Pletzer, L. Koduvelikulathu, C. Comparotto, R. Kopecek, H. Kurz, "Analysis of the annual performance of bifacial modules and optimization methods," *IEEE Journal of Photovoltaics*, vol. 5, no. 1, pp. 320–328, 2015, doi: 10.1109/JPHOTOV.2014.2364406.

[28] M. Vimala, G. Ramadas, M. Perarasi, A. Manokar, R. Sathyamurthy, "A review of different types of solar cell materials employed in bifacial solar photovoltaic panel," *Energies*, vol. 16, no. 8, 2023, doi: 10.3390/en16083605.

[29] M. Abdelkader, "Development and characterization of photovoltaic cells based on Si-mc multicrystalline silicon," *University of Science and Technology Houari Boumediene*, 2017, doi: 10.13140/RG.2.2.18179.99363.

[30] A. Abdallah, M. Kivambe, B. Aïssa, B. Figgis, "Performance of monofacial and bifacial silicon heterojunction modules under desert conditions and the impact of PV soiling," *Sustainability*, vol. 15, no. 10, 2023, doi: 10.3390/su15108436.